Optimizing smartphone-based canopy hemispherical photography

*Gastón Mauro Díaz[a,b]

[a]National Scientific and Technical Research Council —Argentina (CONICET); [b]Patagonian Andes Forest Research and Extension Center (CIEFAP)

*Corresponding author: gdiaz@correociefap.org.ar; Department of Geomatics, CIEFAP, Ruta 259 km 16.24, postal code 9200, Esquel, Argentina

Running headline: Smartphone-based canopy hemispherical photography

Abstract

1) Hemispherical photography (HP) is a long-standing tool for forest canopy characterization. Currently, there are low-cost fisheye lenses to convert smartphones into high-portable HP equipment; however, they cannot be used whenever since HP is sensitive to illumination conditions. To obtain sound results outside diffuse light conditions, a deep-learning-based system needs to be developed. A ready-to-use alternative is the multiscale color-based binarization algorithm, but it can provide moderate-quality results only for open forests. To overcome this limitation, I propose coupling it with the model-based local thresholding algorithm. I call this coupling the MBCB approach.

2) Methods presented here are part of the R package CAnopy IMage ANalysis (caiman), which I am developing. The accuracy assessment of the new MBCB approach was done

with data from a pine plantation and a broadleaf native forest.

3) The coefficient of determination (R^2) was greater than 0.7, and the root mean square error (RMSE) lower than 20 %, both for plant area index calculation.

4) Results suggest that the new MBCB approach allows the calculation of unbiased canopy metrics from smartphone-based HP acquired in sunlight conditions, even for closed canopies. This facilitates large-scale and opportunistic sampling with hemispherical photography.

Key-words: image processing, canopy image, leaf area index, lens calibration

Introduction

Canopies are often characterized with the leaf area index (LAI), defined as one half the total photosynthetic area per unit of horizontal ground surface area (Chen & Black, 1992). Among the established techniques for LAI measurement (Calders et al., 2018), hemispherical photography (HP) is often chosen because of its low purchasing cost and enthusiastic supporting community.

Each HP application requires a balance between sampling density and sample accuracy. Heterogeneos canopies require large sampling efforts (Díaz et al., 2021), while monitoring phenology, high accuracy (Lang et al., 2017). Other applications require opportunistic sampling, common in regions with low terrestrial accessibility. However, most research faces the accuracy problem and little is known about solutions for large-scale and opportunistic sampling.

Error sources for traditional processing protocols are (1) acquiring photographs in non-

diffuse light conditions and (2) wrong exposure settings; besides, independent from the processing protocol, there is improper lens calibration (Fournier & Hall, 2017). These error sources are often combined when HP is used without due training. This is more common now than ever since cheap fisheye lenses are available to convert smartphones in HP equipment.

With the easily available free HP software packages, wrong results can be produced if incorrect parameters are set, such as erroneous lens parameters. Among the free software, CAN-EYE is the most complete since it solves from lens calibration to canopy indices calculation (https://www6.paca.inrae.fr/can-eye/). Other packages tend to focus on a particular link of the processing chain. For instance, CIMES can calculate a wide variety of well-documented canopy indices (Gonsamo et al., 2011), and the R package CAnopy IMage ANalysis (caiman) includes original binarization algorithms (Díaz et al., 2021).

In 2016, I started the development of the 'caiman' package to distribute the multiscale color-based binarization (MCB) algorithm (Díaz & Lencinas, 2015). Later, I introduced the model-based local thresholding (MBLT) algorithm (Díaz & Lencinas, 2018) and, driven by user demands, I expanded some functionalities, such as full-frame support (Bianchi et al., 2017) and adaptive binarization (Martin et al., 2020). Altrought the first proof of concept suggesting that the package can process smartphone-based HP was already published (Bianchi et al., 2017), I have refined important details so a document accounting for those changes is needed. Also, I believe that the calibration of fisheye lenses for smartphones has been overlooked since they tend to strongly deviate from the standard projections. Here I contribute to amending that.

The MCB algorithm was developed to process photographs acquired in sunny days (sunlight images) —a particular non-diffuse light condition— and to mitigate the blooming effect,

linked to incorrect exposure settings (Díaz & Lencinas, 2015). However, a recent evaluation suggests that MCB's sensitivity to exposure is so high that hinders its operational use for closed canopies (Díaz et al., 2021). Till now, the deep-learning (DL) approach by Díaz et al. (2021) is the only available solution for processing sunlight images with sound accuracy. But, its implementation is time-consuming and requires DL know-how.

Here, I propose to couple the MBLT and MCB algorithms (hereafter, MBCB approach). This new workflow is computational demanding but here I show that it has the potential to provide unbiased results for both broadleaf and coniferous woods, requiring only basic knowledge of R scripting. The purpose of this paper is twofold: to present the MCBC approach and to evaluate it with a dataset involving both smartphone-based and regular HP.

Lens calibration

Canopy hemispherical photographs are mostly taken pointing to the zenith. Given that, the vertical line at the lens location is the optical axis. The angle between the optical axis and any other line passing through the lens is the zenith angle (θ). As isolines in a map, points in the image with the same θ form a circle; therefore, each θ has a corresponding radius. The radius expressed as a fraction of the radius for 90º θ is the relative radius (R). Following a standard method, the 'caiman' package uses a polynomial curve to model the relation between θ and R. The fitted model is called a lens projection function.

Based on Clark & Follin (1988), I developed a method to estimate projection coefficients that only requires inexpensive everyday materials: printing an A1 size PDF provided along with the package, a tripod, a table, a standard yoga mat, and push pins of different colors. I programmed the *calibrate_lens()* function for the required calculations. Fig. 1 shows the FC-E9 lens projection function obtained with this method against the validated version. Details

about the latter can be found in Díaz & Lencinas (2018) S3. Also, Fig. 1 shows the projection function of fisheye lenses for smartphones that I found in the Argentinian market.

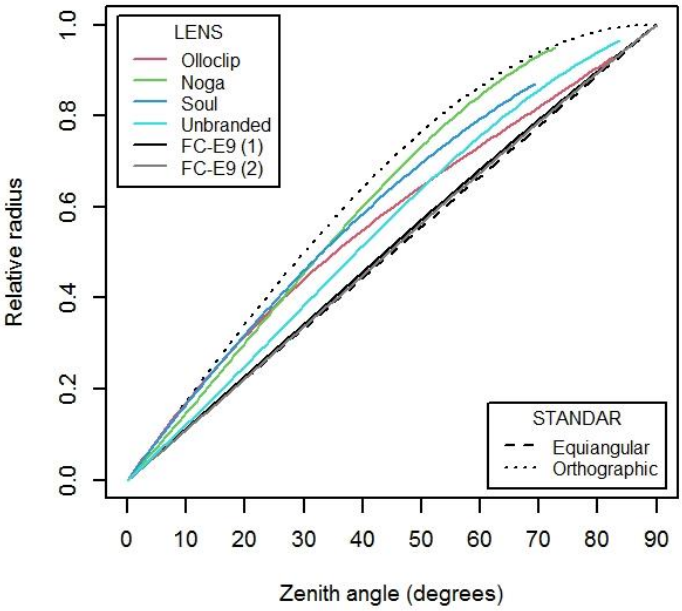

Fig. 1. Lens projection functions of one smartphone lens with long-term market presence (Olloclip), three generic smartphone lenses (Noga, Soul, and Unbranded), and two versions for the well-established FC-E9 lens: (1) validated, and (2) adjusted with the method presented here. For comparison, two standard projections.

Photograph acquisition

Fig. 2 helps understanding the different kinds of photographs that can be acquired and what is the best processing alternative for them. If sampling with high accuracy is needed, then diffuse-light images acquired with professional equipment should be used. For smartphone-based HP (i.e., for non-professional equipment), the acquisition of diffuse-light images can

happen since some regions have a high frequency of overcast days, but sunlight conditions are more likely to occur. Sunlight allows short shutter speeds, ideal to proceed without a tripod. The use of the spirit level built-in feature of smartphones is recommended.

Direct sunlight entering the lens should be avoided. These methods help to achieve it: (1) using the canopy itself to cast a shadow on the lens and (2) use a device to cast a shadow (Kuusk & Paas, 2007). The former is suitable for opportunistic sampling while the latter for rigorous systematic sampling.

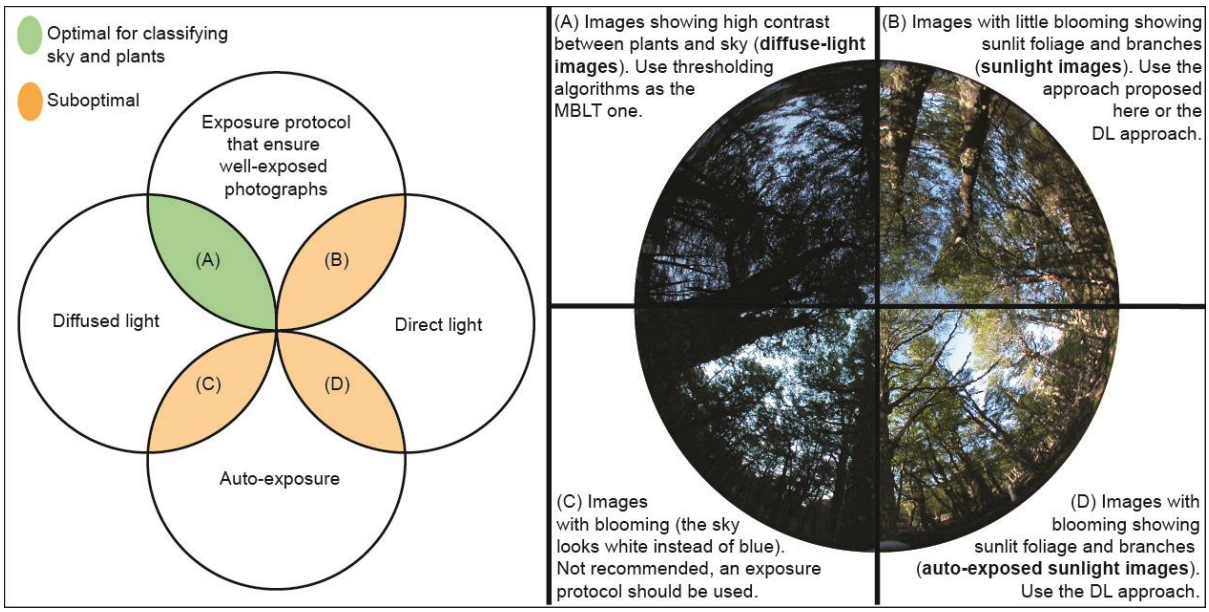

Fig. 2. Relation between camera exposure and light conditions. (C) and (D) are not observed in open canopies because the auto-exposure method provides a result similar to an exposure protocol. The photographs were taken in a *Nothofagus pumilio* forest with a FC-E9 lens (see Fig. 1). MBLT stands for model-based local thresholding, MCB for multiscale color-based binarization, and DL for deep learning.

Evaluation of the MBCB approach

Methods

Two pieces of equipment were used to acquire the hemispherical photographs; a Nikon FC-E9 fisheye converter attached to a Nikon Coolpix 5700 camera, which produces circular fisheye photographs with 1490 pixel diameter at 180º field of view (FOV) —equivalent to 745 pixel radius for 90º θ—; and a Olloclip lens attached to an iPhone 6 Plus, which produces an incomplete circular image (Fig. 3) with 165º diagonal FOV, 160º horizontal FOV, and 110º vertical FOV. Its lens projection is $R = 1.06065\theta - 0.49054\theta^2 + 0.14044\theta^3$ (Fig. 1). The extrapolated radius for 90º θ is 1786 pixels. That is 2.4 times greater than the FC-E9 radius; however, since strong blurring occurs in the Olloclip lens after 55º θ, more pixels is not equivalent to more sharpness.

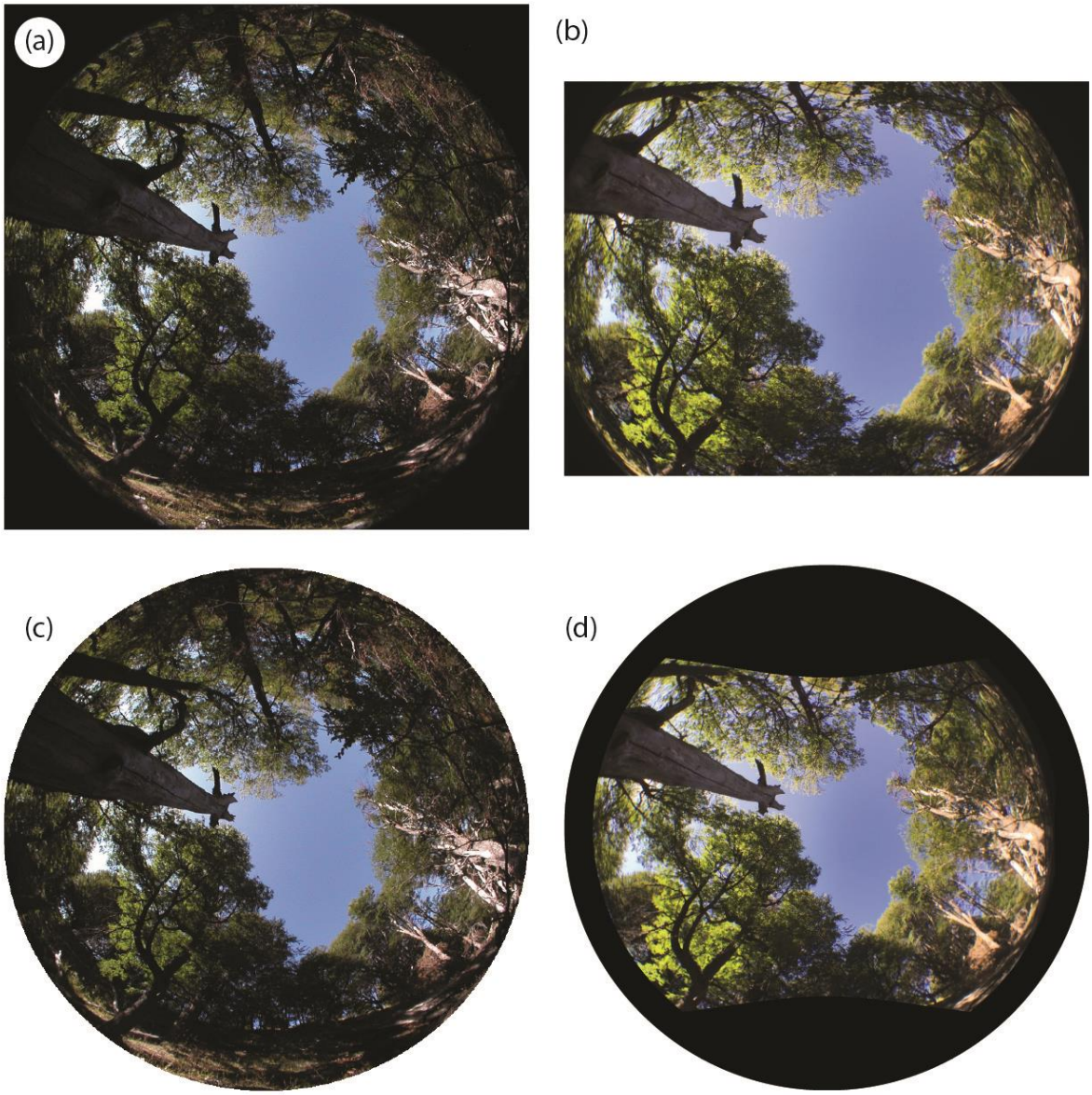

Fig. 3. Original —(a) and (b)— and reprojected —(c) and (d)— canopy hemispherical photographs of a *Pinus ponderosa* plantation. Both reprojected to the equiangular projection. (a) and (c) taken with the FC-E9 lens; (b) and (d), with the Olloclip lens.

Two datasets were used; the one described in Díaz et al. (2021) section 2.1.3, from a native *Nothofagus pumilio* forest (broadleaf species); and another presented here for the first time, from a *Pinus ponderosa plantation*.

The broadleaf forest dataset was acquired in February 2020, in the Huemules Norte experimental unit (42º46′47″ S, 71º27′53″ W). On 104 locations (photosites), two sunlight photograph was taken, one with the FC-E9 lens and another with the Olloclip. To calculate reference values, we used the DL system from Díaz et al. (2021) and the sunlight FC-E9 images to obtain plant area index (PAI) and effective PAI (PAIe), two canopy indices strongly related to LAI.

New data were acquired in a pine plantation near the city of Esquel, Argentina (42º53′49.4″ S, 71º21′36.5″ W), on September 9th, 2020. At dawn, diffuse-light images (FC-E9 lens) were acquired following the same protocols used by Díaz & Lencinas (2018). Fithteen diffuse-light images were acquired along a transec selected to maximize canopy openness variability. Each photosite was flagged. Sunlight images (FC-E9 and Olloclip lenses) were acquired in those photosites in the morning (one missing photo), midday, and afternoon. Sun elevation was 25º, 41º, and 36º, respectively. All of these photographs were taken at 1.25 m from the floor. To calculate the reference values, I binarized the diffuse-light images with the MBLT algorithm and ingested them in the Hemisfer 3.1 software package (https://www.schleppi.ch/patrick/hemisfer). Only the range from 20º to 70º θ was used in the calculations. See Díaz & Lencinas (2018) for more methodological details.

The Olloclip images were acquired with auto-exposure, except when abundant saturation and blowing were observed on the smartphone screen. Then, the exposure was manipulated to diminish it. The FC-E9 sunlight images were always acquired in RAW format and underexposing 1 to 2 stops relative to the on-site auto-exposure, following Beckschäfer et al. (2013). The RAW files were converted into 16-bit TIFFs with the ViewNX-i software by Nikon. For testing, three image versions were produced by modifying the exposure compensation parameter from 0 (default) to 1 and -1.

Sunlight images were binarized with the MBCB approach. Since this article aims at researchers not specialized in HP, the general-purpose binarization algorithm by Ridler & Calvard (1978), known as ISODATA, was also used to serve as a common baseline. From the binarized sunlight images, PAIe and PAI were calculated with Hemisfer as done for the binarized diffuse-light images.

Results and discussion

The pine plantation showed maximum reference values lower than the broadleaf forest (1.2 to 2.8 PAIe and 3.3 to 5.6 PAI vs. 1.1 to 4.9 PAIe and 2.9 and 7.3 PAI). Sunlight images from the former allowed accurate PAIe and PAI calculation, but for the latter, only accurate PAIe (Table1). As expected, the baseline performed worse than the MBCB approach, being that more evident for the broadleaf forest (Table 1). However, although biased, the baseline showed a good correlation with the reference values for pine PAIe. To interpret this, it is necessary to consider that pine photographs were acquired under a complete clear sky, while broadleaf photographs in days with broken clouds in the morning. Therefore, it is uncertain if the type of canopy or the sky conditions affected these correlations. However, based on Fig. 4b (see next paragraph), seems to be the former.

Difference in the solar disk position introduced a random error (Fig. 4a), so repeated measurement with hours of difference could increase accuracy. The source of random error is probably related to variations in the amount of sunlit canopy depicted in the photographs, which depends on the solar disk position and the canopy itself. This could explain the absence of an optimal solar elevation. The lack of difference between morning and afternoon in Fig. 4b might suggest that broken clouds, only presented in the morning, did not affect the results, but further research is needed.

Table 1. Accuracy assessment of both plant area index (PAI) and effective PAI (PAIe) calculated from sunlight hemispherical photographs binarized with the new workflow (MBCB approach) and a baseline (ISODATA algorithm). RMSE stands for root mean square error, R^2 for coefficient of determination and EC for the exposure compensation parameter used to develop the RAW files. Bold type indicates best performing.

			Pine plantation				Broadleaf native forest			
			PAIe		PAI		PAIe		PAI	
Lens	EC	Method	RMSE (%)	R^2	RMSE (%)	R^2	RMSE (%)	R^2	RMSE (%)	R^2
FC-E9	-1	MBCB	8	0.92	13	0.55	26	0.70	28	0.17
FC-E9	0	MBCB	**6**	**0.95**	**8**	**0.77**	23	0.58	23	0.03
FC-E9	1	MBCB	13	0.87	17	0.57	27	0.41	29	0.00
Olloclip	-	MBCB	14	0.82	14	0.47	**20**	**0.72**	**21**	**0.13**
Olloclip	-	ISODATA	21	0.84	19	0.42	34	0.32	34	0.08

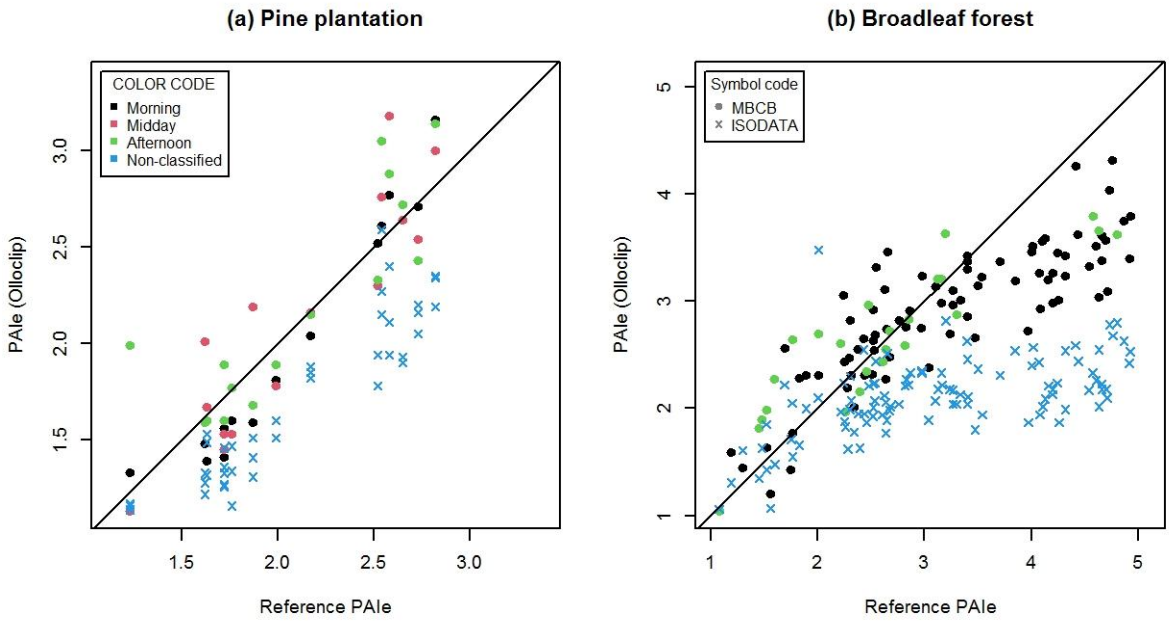

Fig. 4. Accuracy assessment of smartphone-based hemispherical photography in sunlight conditions. PAIe stands for effective plant area index, MBCB for the new approach presented here, and ISODATA is the baseline. Solid lines are the 1:1 relationship.

Varying the EC parameter provided insight for the development of exposure protocols and the potential of the MBCB approach. Based on the calculated errors, I selected the best version of each image and visually analyzed them. It seems that a clear sky depicted in light blue (as it is shown in Fig. 3) should be pursued during photograph acquisition. This protocol is easy to implement with smartphone-based equipment. Regarding the potential of the MBCB approach for supporting PAIe calculation, R^2 and RMSE for the best version of each broadleaf image were 0.87 and 14 %, respectively. And, no bias was observed in the higher values.

The future of the 'caiman' package

The package is evolving as more research is done and users provide feedback. This paper might lead to many new users and a consequent consolidation of its main features. After that, my goal is to conduct a complete reengineering of the package to improve its usability, polish the code, rename it as 'rcaiman', and submit it to the main repository for R packages, the Comprehensive R Archive Network (CRAN).

Conclusion

Smartphone cameras, besides its low-cost and universality, are not inherently superior to other digital cameras used for HP. The same error sources valid for digital HP are valid for smartphone-based HP. Acquisitions in sunlight conditions are common in large-scale and opportunistic sampling, which benefit from the portability of smartphones. I recommend manipulating the exposure to produce sunlight images with the clear sky depicted in light blue. A ready-to-use solution for binarizing sunlight images was presented, which I call the MBCB approach. Although further evaluation is recommended, results suggest that this new solution allows the calculation of unbiased PAIe with smartphone-based HP acquired in sunlight conditions.

Acknowledgements

I thank Veronica Verano for language help.

Data accessibility

The ‘caiman’ package is available in a GitHub repository (https://github.com/GastonMauroDiaz/caiman).

The new workflow (the MBCB approach) is available as a script in a Gist repository (https://gist.github.com/GastonMauroDiaz/1b5962c7e4c2ccebe4c6e4223a19fba1).

Data are available in an OSF repository (https://osf.io/atywm/)

References

Beckschäfer, P., Seidel, D., Kleinn, C., & Xu, J. (2013). On the exposure of hemispherical photographs in forests. *iForest - Biogeosciences and Forestry*, *6*(4), 228–237. https://doi.org/10.3832/ifor0957-006

Bianchi, S., Cahalan, C., Hale, S., & Gibbons, J. M. (2017). Rapid assessment of forest canopy and light regime using smartphone hemispherical photography. *Ecology and Evolution*, *7*(24), 10556–10566. https://doi.org/https://doi.org/10.1002/ece3.3567

Calders, K., Origo, N., Disney, M., Nightingale, J., Woodgate, W., Armston, J., & Lewis, P. (2018). Variability and bias in active and passive ground-based measurements of effective plant, wood and leaf area index. *Agricultural and Forest Meteorology*, *252*, 231–240. https://doi.org/https://doi.org/10.1016/j.agrformet.2018.01.029

Chen, J. M., & Black, T. A. (1992). Defining leaf area index for non-flat leaves. *Plant, Cell & Environment*, *15*(4), 421–429. https://doi.org/10.1111/j.1365-3040.1992.tb00992.x

Clark, J. A., & Follin, G. M. (1988). A simple “equal area” calibration for fisheye photography. *Agricultural and Forest Meteorology*, *44*(1), 19–25. https://doi.org/https://doi.org/10.1016/0168-1923(88)90030-5

Díaz, G. M., & Lencinas, J. D. (2018). Model-based local thresholding for canopy hemispherical photography. *Canadian Journal of Forest Research*, *48*(10), 1204–1216. https://doi.org/10.1139/cjfr-2018-0006

Díaz, G. M., & Lencinas, J. D. (2015). Enhanced gap fraction extraction from hemispherical photography. *IEEE Geoscience and Remote Sensing Letters*, *12*(8), 1785–1789. https://doi.org/10.1109/LGRS.2015.2425931

Díaz, G. M., Negri, P. A., & Lencinas, J. D. (2021). Toward making canopy hemispherical photography independent of illumination conditions: a deep-learning-based approach. *Agricultural and Forest Meteorology*, *296*, 108234. https://doi.org/https://doi.org/10.1016/j.agrformet.2020.108234

Fournier, R. A., & Hall, R. J. (Eds.). (2017). *Hemispherical photography in forest science: Theory, methods, applications*. Springer Netherlands. https://doi.org/10.1007/978-94-024-1098-3

Gonsamo, A., Walter, J.-M. N., & Pellikka, P. (2011). CIMES: A package of programs for determining canopy geometry and solar radiation regimes through hemispherical photographs. *Computers and Electronics in Agriculture*, *79*(2), 207–215. https://doi.org/https://doi.org/10.1016/j.compag.2011.10.001

Kuusk, A., & Paas, M. (2007). Radiometric correction of hemispherical images. *ISPRS Journal of Photogrammetry and Remote Sensing*, *61*(6), 405–413.

https://doi.org/https://doi.org/10.1016/j.isprsjprs.2006.10.005

Lang, M., Nilson, T., Kuusk, A., Pisek, J., Korhonen, L., & Uri, V. (2017). Digital photography for tracking the phenology of an evergreen conifer stand. *Agricultural and Forest Meteorology*, *246*, 15–21. https://doi.org/https://doi.org/10.1016/j.agrformet.2017.05.021

Martin, D. A., Wurz, A., Osen, K., Grass, I., Hölscher, D., Rabemanantsoa, T., Tscharntke, T., & Kreft, H. (2020). Shade-tree rehabilitation in vanilla agroforests is yield neutral and may translate into landscape-scale canopy cover gains. *Ecosystems*. https://doi.org/10.1007/s10021-020-00586-5

Ridler, T., & Calvard, S. (1978). Picture thresholding using an iterative selection method. *IEEE Transactions on Systems, Man, and Cybernetics*, *8*(8), 630–632. https://doi.org/10.1109/tsmc.1978.4310039